Current Biology 20, 259–264, February 9, 2010 ©2010 Elsevier Ltd All rights reserved DOI 10.1016/j.cub.2009.12.045

Report

A Role for Separase in the Regulation of RAB-11-Positive Vesicles at the Cleavage Furrow and Midbody

Joshua N. Bembenek,[1,2,*] John G. White,[1] and Yixian Zheng[2]

[1]University of Wisconsin-Madison, Laboratory of Molecular Biology, 1525 Linden Drive, Madison, WI 53706, USA

[2]Department of Embryology, Carnegie Institution of Washington, and Howard Hughes Medical Institute, 3520 San Martin Drive, Baltimore, MD 21218, USA

Summary

Cell division requires coordinated regulation of chromosome segregation and cytokinesis. Although much is known about the function of the protease separase in promoting sister chromosome separation, the role of separase during cytokinesis is unclear. We show that separase localizes to the ingressing furrow and midbody during cytokinesis in the *C. elegans* embryo. Loss of separase function during the early mitotic divisions causes cytokinesis failure that is not due to eggshell defects or chromosome nondisjunction. Moreover, depletion of separase causes the accumulation of RAB-11-positive vesicles at the cleavage furrow and midbody that is not a consequence of chromosome nondisjunction, but is mimicked by depletion of vesicle fusion machinery. Collectively, these data indicate that separase is required for cytokinesis by regulating the incorporation of RAB-11-positive vesicles into the plasma membrane at the cleavage furrow and midbody.

Results and Discussion

Localization of Separase to the Cleavage Furrow and Midbody during Cytokinesis

We previously found that the *C. elegans* separase SEP-1 localizes to vesicles and promotes cortical granule exocytosis after fertilization during the first meiotic anaphase. Degranulation is an essential prerequisite for functional eggshell formation in *C. elegans*. Furthermore, separase localizes to the base of the polar body as it is extruded [1]. These findings suggest that separase could directly regulate polar body cytokinesis by influencing membrane trafficking. To investigate whether separase has a general function during mitotic cytokineses in *C. elegans*, we analyzed the localization of GFP::SEP-1 in embryos during mitosis. The GFP::SEP-1 transgene can fully rescue a separase mutation in *C. elegans* (see below) and can therefore be used to report the probable localization of the endogenous separase. During metaphase, we find that GFP::SEP-1 localizes to chromosomes, centrosomes, and in a cloud surrounding the metaphase plate (Figure 1A; Movie S1 available online). During anaphase, separase remains on chromosomes and centrosomes and also spreads along the anaphase spindle (Figure 1B). During cytokinesis, separase appears at the cleavage furrow (Figure 1C) and midbody (Figure 1D). We have confirmed the localization of endogenous separase by immunfluorescence to these same structures (Figure S1).

*Correspondence: bembenek@ciwemb.edu

To study the localization of separase further, we expressed protease-dead GFP-separase (GFP::SEP-1^{PD}) with a point mutation of the catalytic cysteine to serine (C1040S). Interestingly, the mutant protease exhibited a more intense localization at putative sites of separase action as compared to the GFP::SEP-1 during anaphase and cytokinesis. GFP::SEP-1^{PD} accumulated as two bright spots within the centrosome, which are likely to be centrioles. It also accumulated strongly in the central spindle region (Figure 1F; Movie S2). Separase has been implicated in licensing centrosome duplication in anaphase [2, 3] and also regulating spindle dynamics [4, 5]. The enhanced localization of GFP::SEP-1^{PD} to these sites may reflect persistent binding to substrates that are not cleaved. Remarkably, GFP::SEP-1^{PD} also accumulates more prominently on the ingressing furrow and midbody during cytokinesis than the wild-type protein (Figures 1G and 1H), suggesting that separase may also act on substrates at these sites. Therefore, separase exhibits a dynamic localization pattern during mitosis, reminiscent of its localization during meiosis I [1]. The localization of separase to the furrow suggests that it may function during cytokinesis.

Separase Directly Regulates Cytokinesis

Consistent with the notion that separase could regulate cytokinesis, previous reports have shown that inactivation of separase causes cytokinesis failure in *C. elegans* [6]. However, some studies have suggested that cytokinesis failures observed after inactivation of separase in *C. elegans* are indirect and can be rescued if the embryos are mounted in ideal conditions that do not apply osmotic or mechanical pressure during image analysis [6]. We sought to re-evaluate the role of separase in cytokinesis given our finding that separase localizes to the furrow and midbody. We analyzed a number of *sep-1(RNAi)*-treated embryos by live-cell imaging with either differential interference contrast (DIC) or fluorescence microscopy to observe cell division. We also titrated the degree of RNAi depletion to match the phenotype presented in the previous study, which was at an intermediate level of separase depletion observed after 20–30 hr of RNAi feeding. We observed embryos during mitosis with ideal buffer conditions and a hanging drop mount to reduce osmotic and mechanical pressures that might cause cytokinesis failures, as done previously by Siomos et al. These conditions allow for the culture of blastomeres completely stripped of the eggshell [7] and preserve viability of fragile meiotic embryos mounted prior to eggshell formation.

As expected, wild-type embryos divide normally under these conditions and do not display cytokinesis failures (n = 20; Figure 2A). However, *sep-1(RNAi)* embryos exhibited a significant incidence of furrow regression resulting in cytokinesis failure, which occurred prior to the second mitotic division (n = 6/22; Figures 2B and 2E). Similar to WT embryos, we observed several known components properly localized to the midbody in *sep-1(RNAi)* embryos (Figures S2A–S2F), confirming that these embryos form midbodies but then subsequently display furrow regression. Therefore, depletion of separase by RNAi to an extent that results in a similar phenotype as previously reported causes a significant rate of

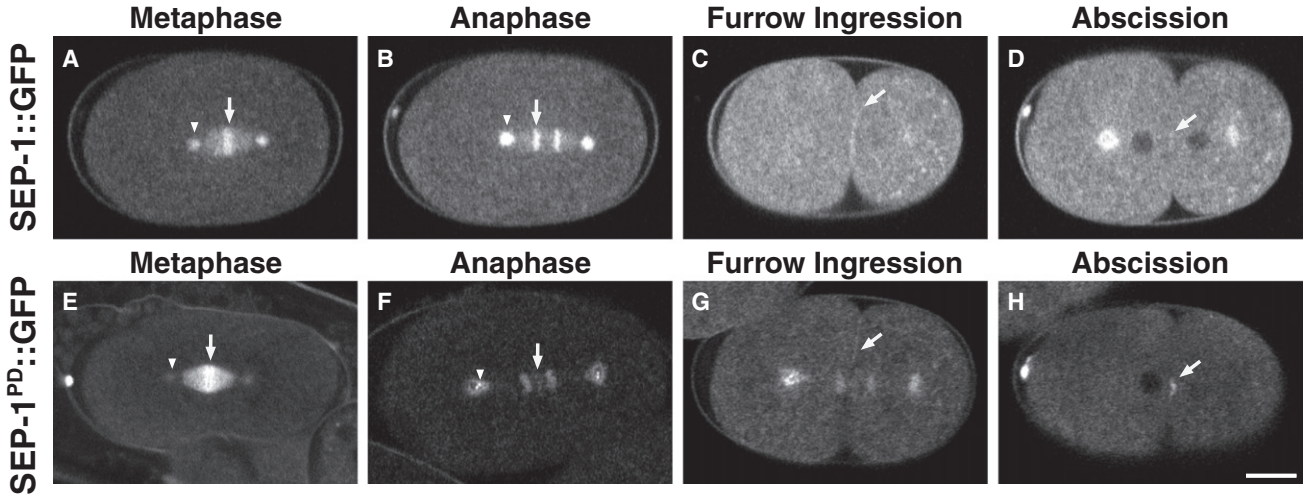

Figure 1. Separase Localizes to the Furrow and Midbody during Cytokinesis

(A) In metaphase, GFP::SEP-1 is observed on chromosomes (arrow), on centrosomes (arrowhead), and on the spindle.

(B) GFP::SEP-1 remains on chromosomes (arrow) and centrosomes (arrowhead) and spreads along the spindle during anaphase.

(C and D) Image at a cortical plane shows a faint localization of GFP::SEP-1 at the furrow (arrow) during cytokinesis (C) and a faint signal is also observed at the midbody (D).

Images in (B)–(D) were captured with elevated laser power and gain settings, because separase signal decreases during anaphase and would otherwise be difficult to illustrate.

(E) GFP::SEP-1^{PD} localizes normally during metaphase.

(F) During anaphase, GFP::SEP-1^{PD} localizes very prominently to two spots within the centrosome (arrowhead), likely centrioles, and the central spindle region (arrow) of the mitotic spindle.

(G and H) During cytokinesis, GFP::SEP-1^{PD} is more prominently observed at the ingressing furrow (G) and midbody (H) (arrows) as compared to GFP::SEP-1.

Scale bar represents 10 μm. See also Figure S1 and Movies S1 and S2.

cytokinesis failures resulting from furrow regression even under optimal mounting conditions.

Separase RNAi also caused chromosome nondisjunction (Figures 2B and 2D). Chromosome nondisjunction has been shown to cause cytokinesis failures in human cells [8]. Recent studies have shown that signaling pathways function in human cells and budding yeast to delay completion of cytokinesis when chromatin is trapped in the midbody [9, 10]. However, many mutations, including those affecting separase and securin, cause the "cut" phenotype in fission yeast where cytokinesis bisects the nucleus, suggesting that not all cell types or mutant conditions fail cytokinesis with chromosome nondisjunction [11]. Nonetheless, it is possible that the furrow regression observed in *sep-1(RNAi)* embryos could be an indirect effect of chromosome nondisjunction in *C. elegans*.

We sought to determine whether the cytokinesis failures we observed as described above are caused by chromosome nondisjunction. We analyzed embryos depleted of the topoisomerase II, *top-2*. As expected, *top-2(RNAi)* caused extensive chromosome nondisjunction (n = 12/12), which persisted for multiple cell divisions in some cases (Figures 2C and 2D). Despite the presence of extensive chromosome bridges, the cytokinetic furrow does not regress (n = 0/12; Figure 2E). This shows that chromosome nondisjunction does not cause cytokinesis failures in the *C. elegans* embryo, consistent with previous studies [12]. As a control, we demonstrated that embryos depleted of both *sep-1* and *top-2* by RNAi display furrow regression (Figure S2G). One caveat of these observations is that depletion of separase, unlike *top-2(RNAi)*, is expected to cause the persistence of cohesin on chromatin, which could indirectly affect cytokinesis. However, the localization of separase to the furrow and midbody taken together with the absence of cytokinesis failure when severe chromosome bridging occurs suggests that separase activity is directly required for cytokinesis. Furthermore, if a checkpoint functions to delay abscission in the *C. elegans* embryo when chromatin is trapped in the midbody, it does not lead to the regression of the furrow within the time window we analyzed. Therefore, cytokinesis failures observed after *sep-1(RNAi)* resulting from furrow regression are probably a result of a direct function of separase during cytokinesis.

To further confirm that separase regulates cytokinesis directly, we analyzed embryos with a temperature-sensitive hypomorphic separase mutation, *sep-1(e2406)*, under ideal mounting conditions. We previously demonstrated that this hypomorph is capable of promoting chromosome segregation, but not cortical granule exocytosis during anaphase of meiosis I [1]. We observed unlabeled embryos with DIC imaging at the restrictive temperature to observe mitosis (Figures 3A–3C). Consistent with our previous observations, nuclei in *sep-1(e2406)* embryos separate normally as observed by DIC (n = 12/17; Figure 3E). We also observed *sep-1(e2406)* embryos expressing labeled histone (H2B::GFP) at 25°C with fluorescent imaging and found that they rarely exhibit chromosome bridging during anaphase (n = 2/20) but they do display lagging chromosomes (n = 11/20; Figure 3J). A significant fraction of the embryos have apparently normal chromosome segregation (n = 6/20). Therefore, the *sep-1(e2406)* mutant does not display as severe chromosome nondisjunction as *sep-1(RNAi)* embryos.

Cytokinesis failures were observed in *sep-1(e2406)* embryos at a higher rate (n = 13/26) than intermediate RNAi depletion, despite having less severe chromosome segregation defects (Figure 3K). Importantly, chromosomal bridges were observed

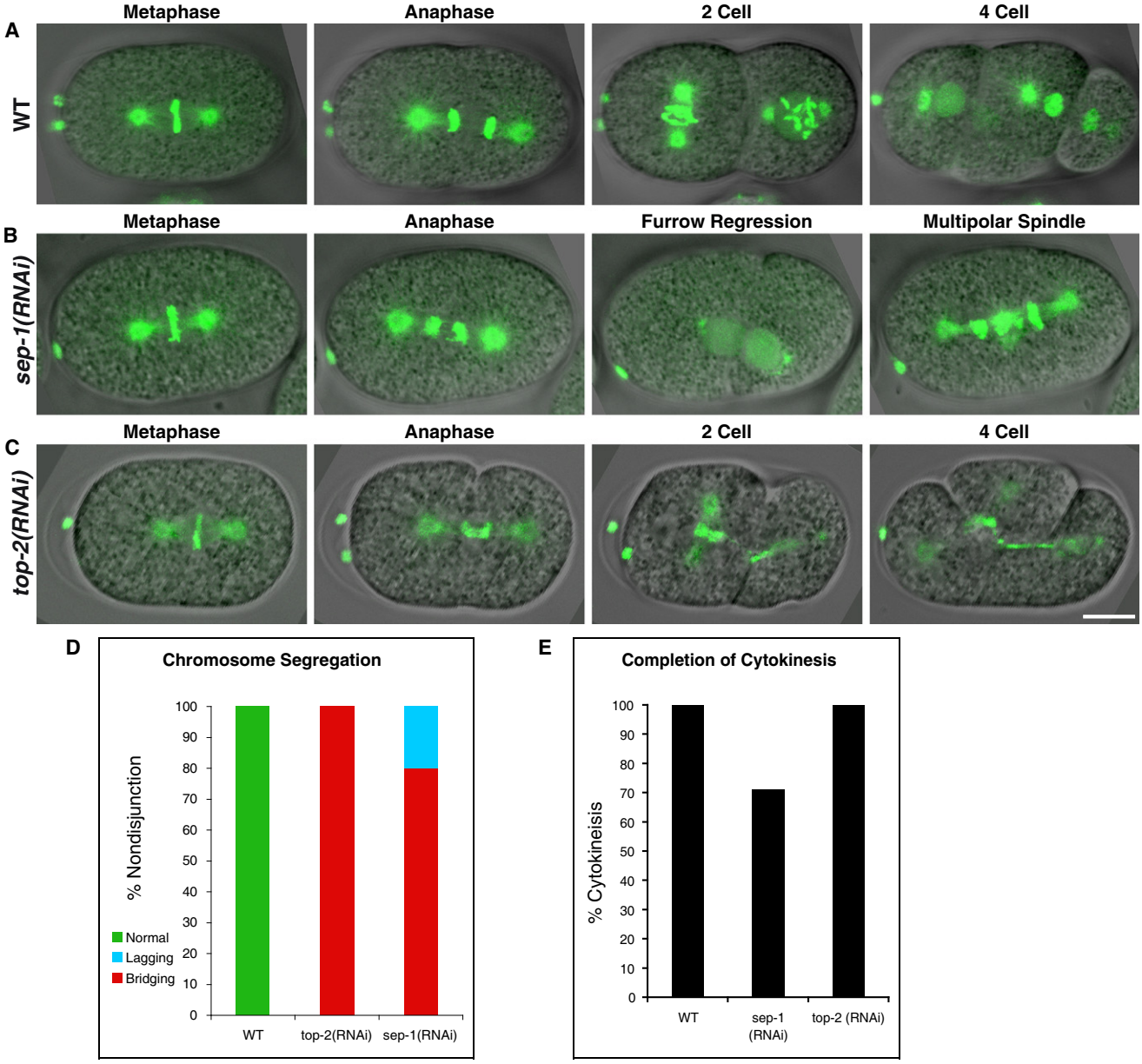

Figure 2. Depletion of Separase Causes Cytokinesis Failures

(A–C) 4D multiphoton images of GFP-histone and -tubulin (green) were maximum z-projected and overlaid with brightfield images (gray).

(A) WT embryos complete the mitotic divisions normally.

(B) Depletion of separase causes chromosome bridges during mitotic anaphase and cytokinesis failures.

(C) Embryos depleted of *top-2* have extensive nondisjunction, leading to persistent chromosome bridges that do not cause furrow regression.

(D) Quantitation of embryos showing normal chromosome segregation, lagging chromosomes, or chromosomal bridging during anaphase.

(E) Although *sep-1(RNAi)* and *top-2(RNAi)* share severe nondisjunction, 28% of *sep-1(RNAi)* embryos, but none of the the *top-2(RNAi)* embryos, display furrow regression.

Scale bar represents 10 μm. See also Figure S2.

in all embryos (n = 6/6) that display cytokinesis failure after *sep-1(RNAi)* treatment, whereas 38% (n = 5/13) of the *sep-1 (e2406)* embryos failing cytokinesis separated their nuclei normally. Therefore, the hypomorphic *sep-1(e2406)* mutation causes cytokinesis failures in the absence of chromosome nondisjunction. Together with the absence of cytokinesis failures after chromosomal bridges are induced by *top-2(RNAi)*, we conclude that separase has a direct role in cytokinesis independent of chromosome segregation.

We also used fluorescent imaging of GFP-histone and membrane dye FM2-10-labeled embryos to more carefully observe chromosome segregation and plasma membrane dynamics during cytokinesis, as done previously [13] (Figures 3G–3I; Movie S3). We observed an abnormal bolus of membrane material at the regressing furrow in *sep-1(e2406)* embryos, indicative of a defect in membrane dynamics during cytokinesis (Figure 3I). Expression of SEP-1::GFP in *sep-1 (e2406)* embryos rescued eggshell defects, chromosome

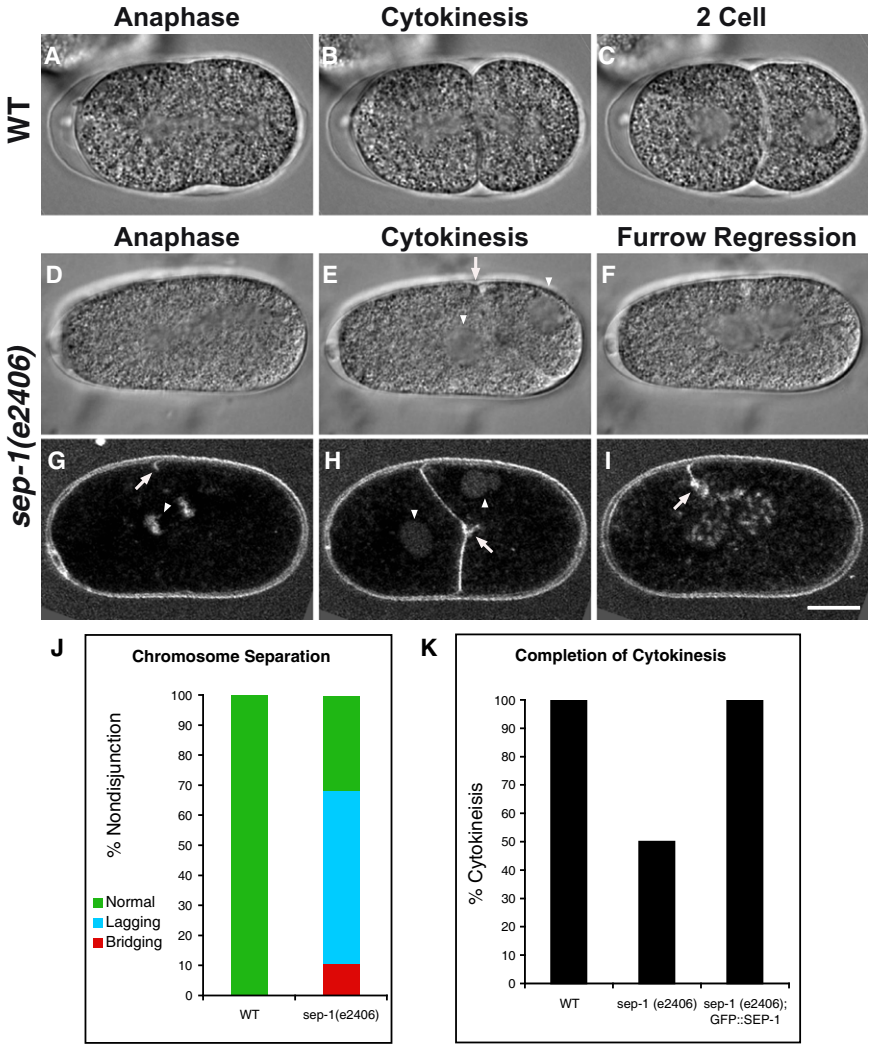

Figure 3. Hypomorphic *sep-1* Mutant Embryos Fail Cytokinesis

(A–C) DIC images of WT embryos during the first mitotic division.

(D–F) *sep-1(e2406)* mutant embryos failing cytokinesis. During anaphase, the nuclei fully separate (arrowheads, E) and the cleavage furrow completes, but later regresses (F).

(G–I) *sep-1(e2406)* mutant embryos labeled with histone-GFP and FM2-10 dye were imaged.

(G) Lagging chromosomes (arrowhead) are observed in anaphase when the furrow (arrow) ingresses.

(H) The nuclei (arrowheads) fully separate when furrowing completes, and some membrane accumulation is observed at the midbody (arrow).

(I) Subsequently, the furrow regresses and a large bolus of membrane material can be observed (arrow).

(J) Quantitation of chromosome separation in *sep-1(e2406)* embryos shows less chromosomal bridging defects than RNAi depletion of separase.

(K) Despite minimal chromosomal bridging, *sep-1(e2406)* embryos have a high rate of cytokinesis failure, which is rescued by the expression of GFP::SEP-1.

Scale bar represents 10 μm. See Figure S3 and Movie S3.

nondisjunction, cytokinesis failures (Figure 3H), and viability. We also took advantage of the temperature sensitivity of the *sep-1(e2406)* allele to shift embryos to the nonpermissive temperature after completion of the meiotic divisions and eggshell formation. We observed furrow regression causing cytokinesis failures in impermeable *sep-1(e2406)* embryos shifted just after eggshell formation (Figure S3). Together, the above studies indicate that inactivation of separase in *C. elegans* causes furrow regression leading to cytokinesis failures independently of meiotic division failures, eggshell permeability, or chromosome nondisjunction.

Separase Regulates the RAB-11-Positive Vesicles during Cytokinesis

To gain insight into the mechanism by which separase promotes cytokinesis, we investigated whether membrane trafficking during mitosis was affected given the abnormal accumulation of FM2-10 labeling at the furrows of *sep-1 (e2406)* embryos during cytokinesis. We focused on studying RAB-11 because of its central role in regulating trafficking and exocytosis of vesicles to the plasma membrane during cytokinesis [14]. For this purpose, we analyzed embryos expressing GFP::RAB-11, previously reported to accurately reflect endogenous localization of RAB-11 [15]. In wild-type embryos, GFP::RAB-11 could be seen in transient patches on the ingressing furrow and weakly accumulated at the midbody during abscission (n = 10/10; Figures 4A, 4E, and 4F; Movie S4). Similarly, embryos depleted of the *top-2* topoisomerase (25–30 hr feeding RNAi) had chromosome bridges but showed no apparent defects in the trafficking of GFP::RAB-11 to the furrow and midbody (n = 8/8; Figures 4B, 4E, and 4F; Movie S5). By contrast, *sep-1(RNAi)* treatment (15–23 hr feeding RNAi) caused prominent and persistent GFP::RAB-11 accumulation at the furrow and midbody during cytokinesis (n = 11/14; Figures 4C, 4E, and 4F; Movie S6). In contrast, we did not observe the accumulation of the early endosomal rab, RAB-5, at the ingressing furrow or midbody during cytokinesis in *sep-1(RNAi)* embryos (Figure S4). Depletion of the plasma membrane-localized t-SNARE (40–64 hr feeding RNAi), *syn-4*, which is also required for cytokinesis in *C. elegans* [16], caused prominent, persistent accumulations of GFP::RAB-11 at the furrow and midbody (n = 6/9; Figures 4D, 4E, and 4F; Movie S7). These data show that regulation of RAB-11-positive vesicles at the ingressing furrow and midbody requires separase, in a similar way that a t-SNARE is required. Therefore, separase is required for cytokinesis and RAB-11 vesicle trafficking at the plasma membrane during cytokinesis in *C. elegans*.

Our observations suggest that separase has a direct role in cytokinesis and regulates the trafficking of RAB-11-positive vesicles during cytokinesis. RAB-11-positive vesicles are known to traffic to the cleavage furrow from a centrosomal pool of recycling endosomes during cytokinesis where they fuse with the plasma membrane to mediate abscission (Figure 4G) [13,17]. The observation of RAB-11-positive vesicle

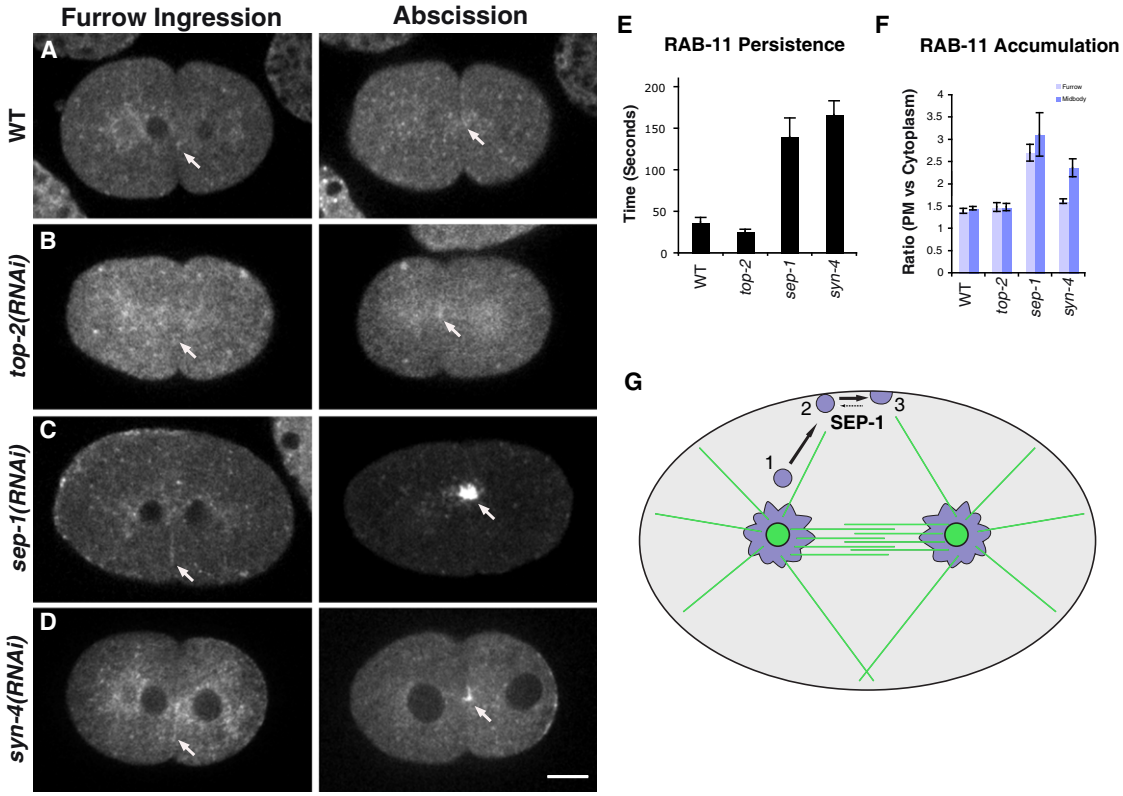

Figure 4. Depletion of Separase Affects RAB-11 Vesicle Trafficking

(A–D) GFP::RAB-11-expressing embryos were imaged during cytokinesis to observe vesicle trafficking at the furrow and midbody (arrows).

(A) During cytokinesis in WT embryos, GFP::RAB-11 puncta can be observed transiently on the ingressing furrow and at the midbody for a short time during early abscission, consistent with its role in regulating vesicle trafficking during cytokinesis.

(B) Depletion of *top-2* causes severe chromosome nondisjunction but does not affect the trafficking of GFP::RAB-11-vesicles to the furrow and midbody during cytokinesis as compared to wild-type embryos.

(C) During furrow ingression in *sep-1(RNAi)* embryos, persistent GFP::RAB-11 localization is observed at the furrow and prominently accumuates at the midbody during abscission.

(D) Depletion of the plasma membrane syntaxin, SYN-4, also causes GFP::RAB-11 to accumulate on the furrow and midbody.

(E) The duration of time that GFP::RAB-11 was observed on the furrow was quantified in embryos showing persistent accumulations during furrow ingression for each condition. Whereas GFP::RAB-11 was observed transiently in WT (37 ± 6 s, n = 5) and *top-2(RNAi)* (26 ± 5 s, n = 4) embryos, it was observed for much longer time in *sep-1(RNAi)* (140 ± 22 s, n = 5, $p < 0.01$) and *syn-4(RNAi)* (166 ± 34 s, n = 4, $p < 0.01$) embryos.

(F) Quantification of the RAB-11::GFP signal in embryos that displayed accumulations of RAB-11 during cytokinesis. To control for variations in signal intensity resulting from z-depth, we calculated the ratio of the intensity of the GFP::RAB-11 signal observed at the furrow (light purple) and midbody (purple) in embryos relative to the average intensity of three equal areas of cytoplasm. The signal ratio in WT embryos at the furrow (1.4 ± 0.05, n = 8) or midbody (1.5 ± .04, n = 8) was similar to the ratios observed for *top-2(RNAi)* embryos (furrow = 1.5 ± 0.09, n = 6; midbody = 1.5 ± 0.08, n = 8). In contrast, both *sep-1(RNAi)* (furrow = 2.7 ± 0.19, n = 6, $p < 0.01$; midbody = 3.1 ± 0.49, n = 9, $p < 0.01$) and *syn-4(RNAi)* (furrow = 1.6 ± 0.05, n = 4, $p = 0.02$; midbody = 2.4 ± 0.2, n = 6, $p < 0.01$) had elevated RAB-11 signal ratios relative to WT embryos. Error bars indicated standard error of the mean.

(G) Proposed model for trafficking of RAB-11-vesicles (purple) during cytokinesis (centrosome and spindle depicted in green). We suggest that at least three steps occur in RAB-11 vesicle trafficking after leaving the recycling endosome: (1) vesicle delivery, (2) tethering, and (3) exocytosis at the plasma membrane. Separase and syntaxin localize to the furrow and cause accumulations of RAB-11-vesicles at the furrow and midbody when depleted, suggesting that vesicles are properly delivered and tethered. We hypothesize that RAB-11 vesicles fail to undergo exocytosis, but their endocytosis (dashed arrow) might also be impaired.

Scale bar represents 10 μm. See Figure S4 and Movies S4–S7.

accumulation at the plasma membrane during cytokinesis is a novel phenotype with respect to RAB-11 trafficking. Other regulators of RAB-11 trafficking have been shown to be important in proper delivery or tethering of vesicles to the cleavage furrow, causing a reduction of vesicles at the plasma membrane when inactivated [18–20]. Our observations that separase localizes to the furrow and midbody and that loss of separase causes an accumulation of RAB-11-positive vesicles at the cleavage furrow and midbody, similar to syntaxin depletion, show that separase is required for a step in RAB-11-positive vesicle trafficking after delivery to the plasma membrane. Given that separase promotes cortical granule exocytosis during anaphase of meiosis I in the *C. elegans* embryo [1], we favor the possibility that separase promotes exocytosis of RAB-11 vesicles during cytokinesis. However, our data cannot rule out the possibility that separase regulates the endocytic recycling of RAB-11 from the plasma membrane after vesicle fusion during cytokinesis. The function of separase in regulation of RAB-11 trafficking may partly explain the furrow regression and failure of cytokinesis we observed in separase RNAi-depleted and mutant embryos. Recently, RAB-11 was also shown to localize to cortical granules and to be required for their exocytosis during anaphase of meiosis I [21]. Therefore, these studies indicate that separase and RAB-11 function

together in a regulatory pathway that coordinates chromosome segregation with membrane trafficking during both meiosis and mitosis in *C. elegans*.

Our findings suggest that separase directly regulates both chromosome separation and cytokinesis during cell division. We show that during mitotic cell divisions, separase first localizes to chromosomes, spreads along the anaphase spindle, and later appears on the cleavage furrow during cytokinesis. This dynamic localization of separase may allow it to coordinate chromosome segregation with membrane trafficking events essential for the success of cytokinesis. The protease activity of separase is also involved in licensing centriole duplication [3] and regulating the spindle during anaphase [4]. Because protease-dead separase accumulates at the centriole, spindle midzone, cleavage furrow, and midbody more than the wild-type protein (Figures 1F–1H), we speculate that separase may proteolyze substrates at each of these cellular locations to coordinate chromosome separation, anaphase spindle dynamics, centrosome duplication, and membrane trafficking during cell division.

Experimental Procedures

Microscopy

Detailed procedures can be found in Supplemental Experimental Procedures. Embryos were mounted in optimized conditions to avoid applying osmotic or mechanical pressure to embryos during microscopy analysis, as previously described [1]. Live cell imaging was performed with a multiphoton system at LOCI (http://www.loci.wisc.edu) as previously described [1] or with a Yokogawa CSU-10 confocal (Newnan, GA, USA).

Statistical Methods

Statistical significance was determined by t test.

Supplemental Information

Supplemental Information includes Supplemental Experimental Procedures, four figures, and seven movies and can be found with this article online at doi:10.1016/j.cub.2009.12.045.

Acknowledgments

We would like to thank Haining Zhang, Erkang Ai, Ahna Skop, Andy Golden, Judy Yanowitz, Geraldine Seydoux, Doug Koshland, Anjon Auhdya, Barth Grant, and members of the Zheng lab for comments, suggestions, and reagents. Kevin Elicieri and Jayne Squirrell at LOCI and Mahmud Siddiqi at Carnegie shared their technical expertise and advice with live cell imaging. This work was supported by an NIH training grant (5F32 GM076867-02) to J.N.B., an NIH grant (R01 GM7583) to J.G.W., and an NIH grant (RO1 GM56312) to Y.Z. Y.Z. is an investigator of the Howard Hughes Medical Institute.

Received: September 9, 2009
Revised: November 15, 2009
Accepted: December 8, 2009
Published online: January 28, 2010

References

1. Bembenek, J.N., Richie, C.T., Squirrell, J.M., Campbell, J.M., Eliceiri, K.W., Poteryaev, D., Spang, A., Golden, A., and White, J.G. (2007). Cortical granule exocytosis in *C. elegans* is regulated by cell cycle components including separase. Development *134*, 3837–3848.
2. Tsou, M.F., and Stearns, T. (2006). Mechanism limiting centrosome duplication to once per cell cycle. Nature *442*, 947–951.
3. Tsou, M.F., Wang, W.J., George, K.A., Uryu, K., Stearns, T., and Jallepalli, P.V. (2009). Polo kinase and separase regulate the mitotic licensing of centriole duplication in human cells. Dev. Cell *17*, 344–354.
4. Baskerville, C., Segal, M., and Reed, S.I. (2008). The protease activity of yeast separase (Esp1) is required for anaphase spindle elongation independently of its role in cleavage of cohesin. Genetics *178*, 2361–2372.
5. Sullivan, M., Lehane, C., and Uhlmann, F. (2001). Orchestrating anaphase and mitotic exit: separase cleavage and localization of Slk19. Nat. Cell Biol. *3*, 771–777.
6. Siomos, M.F., Badrinath, A., Pasierbek, P., Livingstone, D., White, J., Glotzer, M., and Nasmyth, K. (2001). Separase is required for chromosome segregation during meiosis I in *Caenorhabditis elegans*. Curr. Biol. *11*, 1825–1835.
7. Shelton, C.A., and Bowerman, B. (1996). Time-dependent responses to *glp-1*-mediated inductions in early *C. elegans* embryos. Development *122*, 2043–2050.
8. Shi, Q., and King, R.W. (2005). Chromosome nondisjunction yields tetraploid rather than aneuploid cells in human cell lines. Nature *437*, 1038–1042.
9. Steigemann, P., Wurzenberger, C., Schmitz, M.H., Held, M., Guizetti, J., Maar, S., and Gerlich, D.W. (2009). Aurora B-mediated abscission checkpoint protects against tetraploidization. Cell *136*, 473–484.
10. Norden, C., Mendoza, M., Dobbelaere, J., Kotwaliwale, C.V., Biggins, S., and Barral, Y. (2006). The NoCut pathway links completion of cytokinesis to spindle midzone function to prevent chromosome breakage. Cell *125*, 85–98.
11. Funabiki, H., Kumada, K., and Yanagida, M. (1996). Fission yeast Cut1 and Cut2 are essential for sister chromatid separation, concentrate along the metaphase spindle and form large complexes. EMBO J. *15*, 6617–6628.
12. Severson, A.F., Hamill, D.R., Carter, J.C., Schumacher, J., and Bowerman, B. (2000). The aurora-related kinase AIR-2 recruits ZEN-4/CeMKLP1 to the mitotic spindle at metaphase and is required for cytokinesis. Curr. Biol. *10*, 1162–1171.
13. Skop, A.R., Bergmann, D., Mohler, W.A., and White, J.G. (2001). Completion of cytokinesis in *C. elegans* requires a brefeldin A-sensitive membrane accumulation at the cleavage furrow apex. Curr. Biol. *11*, 735–746.
14. Albertson, R., Riggs, B., and Sullivan, W. (2005). Membrane traffic: A driving force in cytokinesis. Trends Cell Biol. *15*, 92–101.
15. Zhang, H., Squirrell, J.M., and White, J.G. (2008). RAB-11 permissively regulates spindle alignment by modulating metaphase microtubule dynamics in *Caenorhabditis elegans* early embryos. Mol. Biol. Cell *19*, 2553–2565.
16. Jantsch-Plunger, V., and Glotzer, M. (1999). Depletion of syntaxins in the early *Caenorhabditis elegans* embryo reveals a role for membrane fusion events in cytokinesis. Curr. Biol. *9*, 738–745.
17. Prekeris, R., and Gould, G.W. (2008). Breaking up is hard to do—Membrane traffic in cytokinesis. J. Cell Sci. *121*, 1569–1576.
18. Rothwell, W.F., Zhang, C.X., Zelano, C., Hsieh, T.S., and Sullivan, W. (1999). The *Drosophila* centrosomal protein Nuf is required for recruiting Dah, a membrane associated protein, to furrows in the early embryo. J. Cell Sci. *112*, 2885–2893.
19. Fielding, A.B., Schonteich, E., Matheson, J., Wilson, G., Yu, X., Hickson, G.R., Srivastava, S., Baldwin, S.A., Prekeris, R., and Gould, G.W. (2005). Rab11-FIP3 and FIP4 interact with Arf6 and the exocyst to control membrane traffic in cytokinesis. EMBO J. *24*, 3389–3399.
20. Ai, E., Poole, D.S., and Skop, A.R. (2009). RACK-1 directs dynactin-dependent RAB-11 endosomal recycling during mitosis in *Caenorhabditis elegans*. Mol. Biol. Cell *20*, 1629–1638.
21. Sato, M., Grant, B.D., Harada, A., and Sato, K. (2008). Rab11 is required for synchronous secretion of chondroitin proteoglycans after fertilization in *Caenorhabditis elegans*. J. Cell Sci. *121*, 3177–3186.